HHS Public Access

Author manuscript

Immunity. Author manuscript; available in PMC 2016 May 19.

Published in final edited form as:

Immunity. 2015 May 19; 42(5): 953–964. doi:10.1016/j.immuni.2015.04.016.

Epidermal fatty acid binding protein promotes high-fat diet-induced skin inflammation

Yuwen Zhang[#1], **Qiang Li**[#1,2], **Enyu Rao**[1], **Yanwen Sun**[1,3], **Michael E. Grossmann**[1], **Rebecca J. Morris**[1], **Margot P. Cleary**[1], and **Bing Li**[1,*]

[1] The Hormel Institute, University of Minnesota, Austin, MN 55912, USA

[2] Department of Burn and Plastic Surgery, Shandong Provincial Hospital Affiliated to Shandong University, Jinan, Shandong, 250021, China

[3] Mayo Clinic Health System, Austin, MN, 55912, USA

[#] These authors contributed equally to this work.

SUMMARY

Defining specific cellular and molecular mechanisms in most obesity-related diseases remains an important challenge. Here we report a serendipitous finding that consumption of a high-fat diet (HFD) greatly increased the occurrence of skin lesions in C57BL/6 mice. We demonstrated that HFD induced the accumulation of a specific type of $CD11c^+$ macrophages in skin preceding detectable lesions. These cells primed skin to induce IL-1β and IL-18 signaling, which further promoted the cytokines IFNγ- and IL-17-mediated skin inflammation. Mechanistically, epidermal fatty acid binding protein (E-FABP) was significantly upregulated in skin of obese mice, which coupled lipid droplet formation and NLRP3 inflammasome activation. Deficiency of E-FABP in obese mice decreased recruitment of $CD11c^+$ macrophages in skin tissues, reduced production of IL-1β and IL-18, and consequently dampened activation of effector T cells. Furthermore, E-FABP deficient mice are completely resistant to HFD-induced skin lesions. Collectively, E-FABP represents a molecular sensor triggering HFD-induced skin inflammation.

INTRODUCTION

Increased food intake and decreased energy expenditure have mainly contributed to the epidemic of obesity worldwide over the past several decades (Hill et al., 2012). Due to the

[*]To whom correspondence should be addressed: Bing Li, The Hormel Institute, University of Minnesota, 801 16th Avenue NE, Austin, MN 55912, USA. Telephone: 507-437-9623. Fax: 507-437-9606. bli@hi.umn.edu.

Disclosure of Potential Conflicts of Interest

The authors state no conflict of interest.

AUTHOR CONTRIBUTIONS

Y.Z. and Q.L. contributed equally to this report. Y.Z., Q.L., E.R., Y.S. and M.E.G. performed the experiments; R.J.M., M.P.C. and B.L. designed the experiments; and B.L. and M.P.C wrote the manuscript, with input from all other authors.

adverse effects of obesity on public health, intensive research has been focused on how obesity is mechanistically linked to metabolic inflammation and various diseases, including type 2 diabetes, cardiovascular diseases and certain types of cancer (Gregor and Hotamisligil, 2011). Mounting evidence has indicated that inflammasome-activated IL-1β and IL-18 responses are essential in promoting obesity-induced inflammation and insulin resistance (Stienstra et al., 2010; Vandanmagsar et al., 2011b). However, it remains to be determined whether the inflammasome-activated signaling represents a general mechanism for other obesity-related diseases.

Fatty acid binding proteins (FABPs) are a group of intracellular chaperones coordinating lipid trafficking and biological functions (Furuhashi and Hotamisligil, 2008; Chmurzynska, 2006). FABPs have traditionally been named according to the tissue in which they were originally identified, such as adipose FABP (A-FABP) or epidermal FABP (E-FABP; encoded by *Fabp5*), but their actual expression profiles and functions are more complicated than previously thought (Smathers and Petersen, 2011). For example, we have demonstrated that E-FABP, beyond being present in keratinocytes in skin epidermis, is widely expressed in immune cells, including T cells and macrophages, where it regulates their immunological functions (Li et al., 2009; Zhang et al., 2014). It has been shown that dietary fatty acids (FAs) can induce the production of IL-1β and IL-18 through activating the NLRP3 (nucleotide-binding domain, leucine-rich repeats containing family, pyrin domain-containing-3) inflammasome pathway in macrophages from HFD-induced obese mice (Wen et al., 2011). Due to the central roles of FABPs in facilitating fatty acid transport and metabolism, it is very likely that FABPs play a critical role in regulating obesity-induced inflammasome signaling.

In our experiments with HFD-induced models of obesity using C57BL/6 mice, we have been frequently notified by the veterinary staff to euthanize obese mice due to skin lesions. Although aged mice with C57BL/6 genetic background are known to be susceptible to inflammatory skin lesions, such as ulcerative dermatitis (Kastenmayer et al., 2006; Williams et al., 2012), a high incidence of skin lesions observed only in the obese mice in our experimental settings clearly suggests that, besides genetic factors, the HFD significantly contributes to skin inflammation. Given the unknown etiology of ulcerative dermatitis syndrome in mice (Duarte-Vogel and Lawson, 2011; Sundberg et al., 2011), and the poor understanding of obesity-associated inflammatory skin diseases in human (Yosipovitch et al., 2007; Shipman and Millington, 2011; Scheinfeld, 2004; Mathur and Goebel, 2011; Mirmirani and Carpenter, 2014), we set out to dissect the cellular and molecular mechanisms of how the HFD, as a major environmental factor, promotes inflammatory skin lesions. Here, we provide evidence to establish E-FABP as a new molecular sensor in triggering HFD-induced skin inflammation.

RESULTS

High-fat diet induces inflammatory skin lesions in obese mice

To study diet-induced obesity models, C57BL/6 mice were randomly grouped and fed on a control low-fat diet (LFD, 10% fat) and a high-fat diet (HFD, 60% fat) after weaning, respectively. Body weight was significantly increased in the group on the HFD as compared

to the group on the LFD after three months (Figure 1A). When we continued to maintain these mice on the same diet for six months, mice on the HFD began spontaneously to develop detectable skin lesions (Figure 1B). We found that approximately 40% of the obese mice developed skin lesions after nine months on the HFD, whereas none of mice on the LFD exhibited similar skin problems (Figure 1C). As the base ingredients included in the two diets were identical except for the fat content (Warden and Fisler, 2008), we reasoned that skin lesions in the obese mice were attributed to the high-fat contents in the diet. We further analyzed the incidence of skin lesional mice on various fat content diets and demonstrated that the skin lesions were positively associated with the fat content in the food, namely, the higher fat in the diet, the more skin lesions in the mice (Figure 1D). Histological staining of skin tissues with hematoxylin and eosin showed that inflammatory cells started emerging in the normal skin of obese mice and accumulated in the lesional skin (Figure 1E). Moreover, skin lesions occurred in different locations of the obese mice, including the areas of neck, flank and leg. To further confirm this observation, we deliberately induced skin lesions of LFD- or HFD-fed mice in a felt wheel skin abrasion model. Skin lesions in HFD-fed mice were much severe than those in LFD-fed mice. Altogether, our data clearly indicate that the HFD is a major environmental factor to promote inflammatory skin lesions in both spontaneous and artificial mouse models.

HFD promotes the infiltration of CD11c$^+$ macrophages in skin

To investigate how consumption of the HFD induces inflammatory skin lesions in obese mice, we hypothesized that HFD may alter the phenotype of immune cell populations in skin. First, we analyzed the immune cell profile in skin samples obtained from LFD-fed lean mice and HFD-fed obese mice without skin lesions. There were no or very few B cells, CD8$^+$ T cells and neutrophils in the skin of these mice; CD4$^+$ T cells, NK cells and $\gamma\delta^+$CD3$^+$ T were present in skin but showed no obvious differences between lean mice and obese mice. However, we noticed that CD11c$^+$F4/80$^+$ macrophages were significantly elevated in skin of obese mice (0.57%±0.04) as compared to lean mice (0.27%±0.024) (Figure S1A). Increase of CD11c$^+$F4/80$^+$ macrophage numbers in obese mice was further confirmed when we analyzed the peripheral blood from these mice (Figure S1B). These data indicate that HFD systemically increases CD11c$^+$F4/80$^+$ macrophages and promotes accumulation of this population in skin tissues preceding detectable lesions. As CD11c$^+$F4/80$^+$ macrophages have been shown to infiltrate into adipose tissues to promote inflammation and insulin resistance (Patsouris et al., 2008; Lumeng et al., 2007), it is very likely that this population is responsible for the initiation of skin pathogenesis in HFD-induced obese mice.

We next analyzed tissues from HFD-fed skin lesion mice by focusing on the CD11c$^+$F4/80$^+$ population. Indeed, we found by flow cytometric analysis that these cells were more than 5-fold numerous in lesional skin than in normal skin of LFD-fed mice (Figure 2A). Confocal microscopic analysis clearly showed that these cells accumulated throughout the lesional skin including both epidermis and dermis (Figure 2B). To further characterize these HFD-elevated skin macrophages, we demonstrated that they exhibited a CD11b$^+$ MHC II$^+$ F4/80$^+$ CD11c$^+$ CD103$^-$ CD207$^+$ (langerin) CD301b$^-$ Ly6C$^-$ CD45$^+$ CD206$^-$ CD64$^-$ CD8a$^-$ phenotype (Figure 2C). In addition, enhanced expression intensity of CD11b on

macrophages from the obese mice suggests that they originate from hematopoietic precursors (Schulz et al., 2012). Since these $CD11c^{+}F4/80^{+}$ cells expressed high amounts of MHC class II, exhibiting essential capacity for antigen presentation (Murray and Wynn, 2011; Hume, 2008), we further examined their presence in peripheral lymph organs. Draining lymph nodes (LNs) and the spleen from the skin lesional mice exhibited significantly increased percentage of $CD11c^{+}F4/80^{+}$ macrophages compared to those from normal mice (Figure S1C, S1D). Phenotypically, they exhibited $CD11b^{+}$ $MHCII^{+}$ $F4/80^{+}$ $CD11c^{+}$ $CD103^{-}$ $CD207^{dim}$ $CD301b^{-}$ $Ly6C^{-}$ $CD45^{+}$ $CD206^{-}$ $CD64^{-}$ $CD8a^{+}$ in LNs (Figure S1E), while displaying a $CD11b^{+}$ $MHCII^{+}$ $F4/80^{+}$ $CD11c^{+}$ $CD103^{-}$ $CD207^{dim}$ $CD301b^{-}$ $Ly6C^{-}CD45^{+}$ $CD206^{-}$ $CD64^{+}$ $CD8a^{-}$ phenotype in the spleen (Figure S1F). Of note, there were no obvious changes regarding the percentage of CD11c single positive cells (Figure S1B, S1D), suggesting that $CD11c^{+}F4/80^{+}$ macrophages are specifically upregulated to mediate skin inflammation upon consumption of the HFD.

Upregulation of IL-1β and IL-18 production in HFD-induced lesion skin

To further determine the molecular mechanism underlying the HFD-induced skin inflammation, we first analyzed the overall profiles of inflammatory cytokines and related factors in skin tissues. In HFD-induced spontaneous lesional skin tissues, we found that inflammasome-related cytokines IL-1β and IL-18 were remarkably upregulated as compared to those in normal skin tissues (Table S1, first column), suggesting that inflammasome signaling is involved in the HFD-induced inflammation. Moreover, when we compared cytokine profiles in the lesional skin between lean mice and obese mice in the felt wheel-induced model, we further confirmed that IL-1β and IL-18 were significantly elevated in obese mice (Table S1, second column). Thus, evidence from both spontaneous and artificial models consistently indicates that IL-1β and IL-18, but not other obesity-related cytokines, such as IL-6 or TNFα, were the major responses mediating the HFD-promoted skin inflammation.

To dissect the cellular sources of these cytokines, we separated major populations in the skin, including keratinocytes, $CD11c^{+}F4/80^{+}$ macrophages and γδ T cells, with a flow sorter (Figure S2). In the HFD-induced spontaneous model, IL-1β mRNA was expressed predominantly in $CD11c^{+}F4/80^{+}$ macrophages, lowly in keratinocytes and non-detectably in γδ T cells (Figure 3A). In contrast, IL-18 mRNA was present in both keratinocytes and macrophages, but undetectable in γδ T cells (Figure 3B). Consistently, similar results were observed in the felt wheel-induced skin lesional model (Figure 3C, 3D), confirming that $CD11c^{+}F4/80^{+}$ macrophages are the major source of IL-1β and IL-18 in skin tissues. More importantly, addition of palmitic acid, the most abundant saturated fatty acids (FAs) in the HFD, significantly stimulated LPS-primed $CD11c^{+}$ macrophages to secrete IL-1β and IL-18 proteins, whereas neither LPS nor FAs alone was able to stimulate IL-1β and IL-18 secretion (Figure 3E, 3F), implying that IL-1β and IL-18-mediated skin inflammation requires at least two signals, one from non-sterile environmental factors, the other from consumption of the HFD. Based on these findings and evidence from other documented research (Stienstra et al., 2010; Vandanmagsar et al., 2011a; Hoffman et al., 2004), our results suggest that HFD promotes $CD11c^{+}F4/80^{+}$ macrophages accumulation in skin and facilitates their production

of IL-1β and IL-18 in a non-sterile environment to initiate skin inflammation. In addition, keratinocytes may also be involved in sustaining skin lesions by secretion of IL-18.

HFD-induced lesion mice are associated with enhanced T cell activation

In addition to the upregulation of IL-1β and IL-18, IFNγ and IL-17 were also significantly elevated in lesional skin tissues (Figure 4A). Considering that IL-1β and IL-18 are well-known for promoting Th1- and Th17 cell-mediated responses (Chung et al., 2009; Netea et al., 2010; Joosten, 2010), we further analyzed T cell infiltration and activation in skin lesion mice. The numbers of $CD4^+$ T cells and $CD8^+$ T cells were significantly increased in the lesional skin as compared to the normal skin of LFD-fed mice (Figure 4B), and they were extensively accumulated to the epidermal-dermal interface in the lesion areas (Figure 4C, 4D). In the draining lymph nodes of normal mice most T cells exhibited naïve phenotypes ($CD4^+$ $CD62L^+$ $CD44^-$, $CD8^+$ $CD62L^+$ $CD44^-$), whereas T cells in lymph nodes of mice with skin lesions were switched to apparent effector or memory phenotypes (Figure 4E, 4F). More strikingly, these activated T cells from lesional mice produced 3-4 fold higher amounts of IFNγ than those obtained from normal mice (Figure 4G-4I). In addition, IL-17 production in $CD4^+$ T cells was also higher in lesional mice than in normal mice (Figure 4J). In line with the above observation, T cells in the spleen also exhibited similar phenotypes and cytokine-producing profiles (Figure S3A-S3E), suggesting a systemic activation status of T cells in the HFD-induced lesional mice. Thus, IL-1β and IL-18 may further promote skin inflammation through inducing T cell activation and cytokine production, such as IFNγ and IL-17, in the HFD-fed obese mice.

HFD upregulates E-FABP expression in skin tissues

In search of the underlying mechanisms by which HFD promotes IL-1β and IL-18 production in skin, we reasoned that FABPs are critical regulators as they coordinate fatty acid trafficking and biological responses inside cells (Furuhashi and Hotamisligil, 2008; Chmurzynska, 2006). We first measured the expression profile of the FABP family in skin. As expected, E-FABP was the most predominant form of FABP family in skin (Figure 5A). Importantly, HFD upregulated E-FABP amounts in skin when compared to LFD (Figure 5B). Compared to the skin of LFD-fed mice, more cells isolated from the skin of HFD-fed mice expressed intracellular E-FABP, but not A-FABP (Figure S4A, S4B). Since $CD11c^+$ macrophages were significantly accumulated in skin tissues of HFD-fed mice (Figure S2A), we further separated $CD11c^+$ macrophages and keratinocytes by flow sorting and measured E-FABP expression in these isolated populations. We found that the expression of E-FABP from the HFD-induced obese mice was 2-fold higher in keratinocytes, but 6-fold higher in macrophages, as compared to their respective controls from the LDF-fed lean mice (Figure 5C, 5D). Immunohistochemistry (IHC) staining clearly demonstrated that E-FABP expressed in the top layer of skin epidermis was enhanced in the normal skin of HFD-fed mice and reached a high level in the HFD-induced lesional skin (Figure 5E). Notably, inflammatory macrophages with high E-FABP expression were also extensively infiltrated in the lesional areas (last panel, Figure 5E). In contrast, E-FABP expression in the skin of the felt wheel-induced lesional model exhibited no obvious elevation when compared to the HFD-induced spontaneous model (Figure S4C), suggesting that E-FABP upregulation in the HFD-induced spontaneous lesional model is not secondary to the inflammatory responses.

Altogether, these results suggest that elevated E-FABP in the skin of HFD-fed mice is a critical regulator in promoting HFD-induced skin inflammation.

E-FABP expression promotes inflammasome activation and cytokine production

To assess whether and how E-FABP expression promotes skin inflammation, we first employed *Fabp5*$^{+/+}$ mice and *Fabp5*$^{-/-}$ mice and compared cytokine production by CD11c^{+} macrophages and keratinocytes obtained from these mice. As shown in Figure 6, E-FABP was not present in skin tissues, including both CD11c^{+} macrophages and keratinocytes, of *Fabp5*$^{-/-}$ mice (Figure 6A-6C). When we stimulated bone marrow-derived CD11c^{+} macrophages from *Fabp5*$^{+/+}$ and *Fabp5*$^{-/-}$ mice with either saturated FAs or unsaturated FAs, we found that saturated FAs, but not unsaturated FAs, greatly stimulated LPS-primed *Fabp5*$^{+/+}$ macrophages to produce IL-1β. In contrast, there was significantly less cytokine production in FA-stimulated *Fabp5*$^{-/-}$ macrophages (Figure 6D). We further separated skin CD11c^{+} macrophages from *Fabp5*$^{+/+}$ and *Fabp5*$^{-/-}$ mice and demonstrated that E-FABP deficiency significantly reduced IL-1β production in response to LPS plus FA stimulation (Figure 6E). These observations indicate that E-FABP expression in macrophages is essential in promoting saturated FA-induced cytokine production.

Given the critical role of the inflammasome in governing the activation of IL-1β processing (Fantuzzi and Dinarello, 1999; Petrilli et al., 2007), we next measured NLRP3 expression in saturated FA-stimulated macrophages derived from bone marrow of *Fabp5*$^{+/+}$ and *Fabp5*$^{-/-}$ mice (Figure 6F). Expression of NLRP3 in *Fabp5*$^{+/+}$ macrophages was greatly enhanced above amounts in E-FABP$^{-/-}$ macrophages. In addition, we observed that the enhanced NLRP3 was exactly co-localized with lipid droplets (LDs) inside macrophages. As E-FABP is the major lipid carrier facilitating LD formation in CD11c^{+} macrophages (Zhang et al., 2014), we hypothesized that E-FABP might promote the production of IL-1β by coupling LD formation and NLRP3 inflammasome activation. To this end, we used dietary FAs to stimulate LPS-primed macrophages with the inhibition of LD formation by Triacsin C (Namatame et al., 1999). IL-1β amounts in the cultural supernatants of macrophages stimulated with either saturated FAs or unsaturated FAs were suppressed with the inhibition of LDs (Figure 6G, 6H). Concomitant with these observations in CD11c^{+} macrophages, E-FABP expression was also required for the IL-1β production in keratinocytes (Figure S5A). Moreover, active Caspase-1 was co-localized with LDs in keratinocytes (Figure S5B), and inhibition of LDs also inhibited IL-1β production in keratinocytes (Figure S5C), further suggesting a new function of LDs in facilitating the binding and activation of inflammasomes. Lastly, when we knocked down ASC, a broad inflammasome adaptor, in macrophages with specific ASC siRNA sets, we showed that ASC-knockdown significantly reduced IL-1β production in response to LPS and FA stimulation (Figure S5D-S5F), which was consistent to the results obtained from ASC-deficient mice (Wen et al., 2011). Altogether, our data indicate that E-FABP expression in skin tissues is crucial in coupling the formation of LDs and activation of NLRP3/ASC/Caspase-1 inflammasome, thus revealing E-FABP as a new molecular sensor in fatty acid-induced inflammatory cytokine production.

E-FABP deficiency protects mice against HFD-induced inflammatory skin lesions

Having established the critical role of E-FABP in promoting inflammasome activation and subsequent cytokine production *in vitro*, we further wanted to determine whether E-FABP expression instigates HFD-induced skin inflammation *in vivo*. *Fabp5*$^{+/+}$ and *Fabp5*$^{-/-}$ mice were fed the HFD as described above and were observed for the development of skin lesions. Consistent with previous studies (Maeda et al., 2003), *Fabp5*$^{-/-}$ mice did not display any apparent alterations in subcutaneous adiposity (Figure S6A) or total body weight as compared to *Fabp5*$^{+/+}$ mice (Figure 7A). However, after nine months of the HDF 40% of obese *Fabp5*$^{+/+}$ mice developed inflammatory skin lesions with enlarged spleen and draining lymph nodes, whereas none of *Fabp5*$^{-/-}$ mice exhibited any above symptoms (Figure 7B, Figure S6B and S6C). These results further confirmed that E-FABP expression is decisive for the HFD-induced skin lesions.

While consumption of the HFD promoted the accumulation of CD11c^{+} macrophages in skin of *Fabp5*$^{+/+}$ mice, we found that very few macrophages, in particular CD11c^{+} macrophages, were present in *Fabp5*$^{-/-}$ mice fed the same HFD (Figure 7C), suggesting an essential role of E-FABP in the HFD-induced differentiation of CD11c^{+} macrophages *in vivo*. In line with these observations, serum levels of IL-1β and IL-18 were significantly higher in *Fabp5*$^{+/+}$ mice than those in *Fabp5*$^{-/-}$ mice (Figure 7D, 7E). Thus, E-FABP deficiency alters both macrophage phenotype and their functions. Furthermore, we also measured T cell infiltration and activation in *Fabp5*$^{+/+}$ and *Fabp5*$^{-/-}$ mice and demonstrated that fewer T cells were present in skin epidermis of *Fabp5*$^{-/-}$ mice as compared with *Fabp5*$^{+/+}$ mice (Figure S6D). Importantly, T cells in the draining LNs of *Fabp5*$^{-/-}$ mice produced less IFNγ and IL-17 than cells from *Fabp5*$^{+/+}$ mice (Figure 7F-7H). Similarly, E-FABP deficiency in splenic T cells also impaired their cytokine production (Figure S6E, S6F). We have shown that E-FABP deficiency in T cells has no major impact on IFNγ production (Li et al., 2009), thus, the elevated IFNγ in obese *Fabp5*$^{+/+}$ mice may be attributed to the elevated IL-1β and IL-18 in these mice. Taken together, E-FABP deficiency prevents HFD-induced obese mice from developing skin lesions through altering macrophage phenotype and consequently their functional profiles that promote T cell activation.

DISCUSSION

Obesity has been linked to the development of cardiovascular disease, diabetes and certain types of cancer (Khandekar et al., 2011). However, people seldom think of dermatologic conditions with overnutrition status. Besides obesity-associated physiological alternations of skin, emerging evidence indicates that obesity is positively correlated with bacterial skin infection and inflammatory skin disorders (e.g. pruritus, seborrheic dermatitis) with unknown mechanisms (Mirmirani and Carpenter, 2014). In the present study we demonstrate a clear link between HFD-induced obesity and the induction of inflammatory skin lesions in mouse models.

A frequently used model of obesity which closely mirrors the human situation results from feeding C57BL/6 mice a HFD following weaning. Considering obesity as a chronic disease, we normally keep the mice on the HFD for at least half a year to mimic the long-term effects of elevated body weight. Surprisingly, we noted a high occurrence of skin lesions in the

HFD-fed mice, but not in the LFD-fed littermates in the same environment, which hinted to us that this could be a great model to dissect how excess energy intake interfaces with genetic factors to promote inflammation in skin tissues. In the process of determining cellular sensors which induce skin inflammation, our data suggest a specific phenotype of skin $CD11c^+$ macrophages as a key cellular sensor for the HFD-induced skin inflammation in several aspects. (1) HFD consumption systemically enhanced $CD11c^+$ macrophages in the circulation and promoted their influx in skin tissues before apparent skin lesions in mice. (2) This population was further accumulated in lesion areas to promote skin inflammation through production of proinflammatory cytokines, mainly as IL-1β and IL-18. (3) In addition, *Fabp5*$^{-/-}$ mice with reduced influx of $CD11c^+$ macrophages were fully resistant to skin lesions. In line with our observations, the pathogenic role of $CD11c^+$ macrophages in promoting insulin resistance as well as adipose tissue inflammation in obese mouse models has also been confirmed by other studies (Patsouris et al., 2008; Lumeng et al., 2007; Wentworth et al., 2010).

However, some critical questions are raised along these observations. First, how does consumption of a HFD induce the differentiation of $CD11c^+$ macrophages? We found that E-FABP is specifically expressed in $CD11c^+$ macrophages and its expression levels positively correlate with the intensity of CD11c in macrophages (Zhang et al., 2014). As a major fatty acid carrier, E-FABP was significantly upregulated in macrophages in response to the stimulation of dietary FAs *in vitro* (data not shown) and to consumption of the HFD *in vivo*, which may thus promote CD11c expression to facilitate the uptake and processing of the elevated lipids. In support of this notion, we found that E-FABP deficiency in obese mice displayed reduced CD11c expression in skin macrophages. In addition, we noticed that A-FABP, another FABP family member expressed in macrophages (Makowski et al., 2005), was not present or expressed at very low levels in primary $CD11c^+$ macrophages (unpublished data), further evidencing that it is E-FABP which responds to HFD to regulate CD11c expression in macrophages. The detailed mechanisms of E-FABP-CD11c interactions are currently under investigation.

Secondly, what kinds of factors link HFD to inflammasome activation and IL-1β release in macrophages? The accumulated evidence suggests that the mechanisms involved in these biological events may be multifaceted. For example, saturated FAs in the HFD have been shown to activate the NLRP3 inflammasome through AMPK-autophagy-ROS signaling pathway (Wen et al., 2011), whereas ceramides, fatty acid metabolites, can induce NLRP3-Caspase-1 activation and IL-1β release in macrophages (Vandanmagsar et al., 2011b). Moreover, it is also possible that other lipid components in the HFD, such as cholesterol, can induce inflammasome activation and IL-1 production (Duewell et al., 2010). After carefully analyzing these studies we found one common characteristic among these inflammasome activators from the HFD, insolubility in aqueous environments. In other words, these compounds have to be effectively transported and stabilized in specific niches to activate inflammasomes inside cells. As intracellular FABPs actively bind hydrophobic ligands, facilitating their transport and subsequent responses (Furuhashi and Hotamisligil, 2008; Chmurzynska, 2006; Smathers and Petersen, 2011), it is very likely that E-FABP expression in $CD11c^+$ macrophages may serve as a new link between HFD and

inflammasome activation. Indeed, E-FABP deficiency significantly inhibited FA-induced IL-1β secretion in macrophages. More interestingly, the observations of colocalization of NLRP3 inflammasome with LDs and suppression of IL-1β by LD inhibition imply that E-FABP-mediated LD formation provide a new platform for the effective activation of the inflammasome. Given the unknown cellular localization of inflammasomes and underappreciated functions of LDs (Farese, Jr. and Walther, 2009; Wang et al., 2013), our data suggest a new interaction between inflammasomes and LDs. Thus, E-FABP represents a new molecular link between overnutrition and metabolic inflammation through coupling fatty acid trafficking and inflammasome activation.

Lastly, although saturated FAs are the major components in the HFD, whether other unsaturated FAs contribute to skin inflammation remains unclear. While LPS-primed $CD11c^+$ macrophages produce a large quantity of IL-1β in response to palmitate stimulation, they don't respond to the stimulation of oleate or linoleate, suggesting a marginal effect of unsaturated FAs on IL-1β-mediated skin inflammation. Consistent with our results, unsaturated FAs apart from ω-3 FAs have no obvious effects on NLRP3 activation in macrophages (Yan et al., 2013). Recently, it was reported that high concentrations of unsaturated FAs can even prevent the activation of the NLRP3 inflammsome in macrophages (L'homme et al., 2013). Considering that defective autophagy can lead to inflammasome activation (Nakahira et al., 2011; Wen et al., 2011), increased autophagy caused by unsaturated FAs may partially explain why they can inhibit NLRP3 activation (Mei et al., 2011). Altogether, integration of all evidence indicates that $CD11c^+$ macrophage-mediated chronic skin lesions are mainly induced by the saturated FAs, but not by the unsaturated components, in the HFD.

It is worth noting that E-FABP upregulation, especially in the skin lesional areas, is very striking. This phenomenon was also observed in other skin disorders, such as psoriasis, with unknown mechanisms (Ogawa et al., 2011). We noticed that the HFD slightly enhances γδ T cell proliferation in skin. When we separated γδ T cells with a flow sorter and cocultured them with IL-1β, we found that IL-1β can activate γδ T cells to produce a large amount of keratinocyte growth factor (data not shown), which may promote keratinocyte proliferation and E-FABP expression (Jameson and Havran, 2007; Grau et al., 2006). As discussed above, elevated E-FABP can activate NLRP3-ASC-Caspase-1 inflammasome and subsequent IL-1β and IL-18 processing, which in turn exacerbate skin inflammation by inducing Th1 and Th17 cell adaptive cellular responses (Chung et al., 2009; Netea et al., 2010; Joosten, 2010). Thus, our models support a new concept of collaborative effects between immune cells and local skin cells, in which HFD-induced skin inflammation is initiated by $CD11c^+$ macrophages, sustained by γδ T cells and keratinocytes, and further escalated by adaptive T cells.

In conclusion, the present work reveals a novel mechanism by which consumption of HFD promotes the accumulation of a specific type of $CD11c^+$ macrophages in skin, which prime skin to induce IL-1β and IL-18 signaling in response to environmental stimuli (e.g. LPS), and further contributes to keratinocyte proliferation and effector T cell activation in skin tissues. More importantly, our data demonstrate that the absence of E-FABP, a major lipid carrier in $CD11c^+$ macrophages and keratinocytes, results in complete protection against

HFD-induced skin lesions in mice, thereby establishing E-FABP as a new molecular sensor in HFD-induced skin inflammation. Thus, E-FABP-mediated inflammation may represent a new mechanism contributing to obesity-related inflammatory diseases not only in skin but also in other tissues.

EXPERIMENTAL PROCEDURES

Mice

Fabp5$^{+/+}$ mice and *Fabp5*$^{-/-}$ littermates (C57BL/6 background) were bred and housed in the animal facility in the Hormel Institute in accordance with University of Minnesota Institutional Animal Care and Use Committee (IACUC). All animal protocols were approved by IACUC in University of Minnesota and followed national guidelines. Male mice were fed *ad libitum* with either a HFD (60% fat) or a control LFD (10% fat) (Research Diets) after weaning for 9 months for the observation of spontaneous skin lesions. For artificial induction of skin lesion in lean and obese mice, a felt wheel-induced skin lesion model was performed as we previously described (Hayes et al., 2011). Briefly, mice fed the HFD or LFD for 6 months were anesthetized and removed dorsal back fur. Dorsum of lean and obese mice was equally abraded with a felt wheel on a motor tool. Mice were sacrificed 7 days following the abrasion, and samples were taken for analyses.

Skin cell preparation and stimulation

Dorsal skin from mice was removed and scraped off the subcutaneous fat tissues with the back of the NO. 10 curved scalpel. After thorough rinse, skin was cut into ~ 0.5-1 cm^2 squares and digested with Dispase (1.8u/ml) (Invitrogen) for 60 min at a 37°C incubator with gentle shaking. Epidermis was separated from dermis and further digested in 3ml 0.25% Trypsin/EDTA (Corning Cellgro) in a 37°C incubator for 15 min. After single cells were washed and filtrated through 50μM nylon filters, they were stained with various mAb. Mouse skin $CD11c^+F4/80^+$ macrophages, γδ T cells ($CD3^+$ $\gamma\delta TCR^+$) and keratinocytes ($CD11c^-F4/80^-CD3^-$ $\gamma\delta TCR^-$) were separated with a BD FACSAria II Cell Sorter. Bone marrow-derived $CD11c^+F4/80^+$ macrophages were generated as previously described (Zhang et al., 2014). After skin separated cells or BM-derived $CD11c^+$ macrophages were pretreated with LPS (100ng/ml), they were stimulated with either palmitate (200μM) or oleate/linoleate (200μM) for 20h as indicated. In the experiments with LD inhibition, keratinocytes or macrophages were stimulated with saturated or unsaturated FAs in the presence of absence of lipid droplet inhibitor Triacin C (2 and 5μM). Culture supernatants were collected for ELISA measurements of IL-1β (Biolegend) and IL-18 (MBL International Corporation). Treated cells were analyzed by confocal microscopy or real-time PCR analyses, respectively.

Flow cytometric analysis

Immune cells from skin, peripheral blood (PBMCs), draining lymph nodes and spleens were subjected to surface staining or cultured with PMA (5ng/ml; Sigma), ionomycin (500 ng/ml; Sigma) and Golgiplug (BD) for 6~8 hrs, and harvested for intracellular staining. Flow cytometric data were collected with BD FACS Calibur™ or BD FACSAria II Cell Sorter,

and analyzed by Flowjo (Tree Star). See detailed antibodies in the supplemental information.

Skin immunohistochemistry (IHC) and H&E staining

Skin samples obtained from *Fabp5*$^{+/+}$ or *Fabp5*$^{-/-}$ mice were fixed in 10% neutral buffered formalin or snap-frozen in cryo-embedding media OCT (Sakura Finetechnical Co., Ltd). The paraffin-embedded samples were cut to 5μm sections and stained with hematoxylin and eosin (H&E). For IHC staining, the sections were blocked with ready-to-use (2.5%) normal horse blocking serum and then stained with goat anti-E-FABP antibody (R&D systems) for 1 hour at room temperature. The sections were developed with Immpress Detection System (Vector Laboratories) and counterstained with hematoxylin.

Confocal microscopy

Separated keratinocytes or CD11c^{+} macrophages with designated treatments were cultured on poly-D-lysine coated 12mm coverslips (Neuvitro) in 24-well plates. After treatment, cells were fixed in 3.7% (w/v) formaldehyde in 0.1 M phosphate buffer (pH 7.4) at room temperature for 10 min, then permeabilized in 0.1% Saponin in 1× PBS for 10 min at room temperature for lipid droplet staining using BODIPY® 493/503 (Invitrogen) and/or NLRP3-Caspase-1(Millipore) staining. The nucleus was stained with 0.2μM DAPI (Invitrogen). For skin tissue immunofluorescence staining, frozen sections were blocked and directly stained with anti-CD4, anti-CD8, anti-CD11c, and anti-F4/80 for 40 min at room temperature. Confocal analysis was done with Nikon Eclipse TE2000 confocal microscopy.

Quantitative real time-PCR

For real-time PCR analysis, RNA was extracted from cells using RNeasy Mini Kit (Qiagen). cDNA synthesis was performed with QuantiTect Reverse Transcription Kit (Qiagen). Quantitative PCR was performed with SYBR® Green PCR Master Mix using ABI 7500 Real-Time PCR Systems (Applied Biosystems). Relative mRNA levels were determined using β-actin or HPRT1 as a reference gene. Primer sets other than purchased from Qiagen are listed in the supplemental information.

Western Blotting

For measurement of FABP protein levels in skin tissues, cells from skin epidermis were lysed in buffers with protease inhibitors. For analysis of ASC expression in macrophages, cells were transfected with 200nM ASC siRNA or scramble siRNA (Santa Cruz) using Oligofectamine (Life Technologies) for 24h before cells were collected. Protein concentration was determined by BCA assay (Thermo Scientific). Anti-Mouse E-FABP and A-FABP antibodies (R&D Systems) were used for E-FABP and A-FABP blotting. Anti-ASC antibody (Millipore) was used for measuring ASC expression. β-actin (Cell Signaling) was quantified as a loading control. Image Quant TL system was used for relative protein quantification.

Statistical Analysis

Student t-test and Z-test were utilized for comparison, P-value <0.05 was considered significantly different.

Supplementary Material

Refer to Web version on PubMed Central for supplementary material.

ACKNOWLEGEMETNS

The authors thank Dr. Jill Suttles for providing the E-FABP deficient mice, Dr. Xuan-Mai T. Person and Dr. Michael D. Jensen for fat composition analysis with lipid mass spectrometry. This work was supported by the Hormel Foundation, Minnesota Obesity Center (5P30DK50456), Career Transition Fellowship (NMSS, TA3047-A-1), NIH R01 grants (CA18098601A1, CA17767901A1, CA157012), NIDDK (U24DK100469) and NCATs (UL1TR000135).

REFERENCES

Chmurzynska A. The multigene family of fatty acid-binding proteins (FABPs): function, structure and polymorphism. J. Appl. Genet. 2006; 47:39–48. [PubMed: 16424607]

Chung Y, Chang SH, Martinez GJ, Yang XO, Nurieva R, Kang HS, Ma L, Watowich SS, Jetten AM, Tian Q, Dong C. Critical regulation of early Th17 cell differentiation by interleukin-1 signaling. Immunity. 2009; 30:576–587. [PubMed: 19362022]

Duarte-Vogel SM, Lawson GW. Association between hair-induced oronasal inflammation and ulcerative dermatitis in C57BL/6 mice. Comp Med. 2011; 61:13–19. [PubMed: 21819677]

Duewell P, Kono H, Rayner KJ, Sirois CM, Vladimer G, Bauernfeind FG, Abela GS, Franchi L, Nunez G, Schnurr M, Espevik T, Lien E, Fitzgerald KA, Rock KL, Moore KJ, Wright SD, Hornung V, Latz E. NLRP3 inflammasomes are required for atherogenesis and activated by cholesterol crystals. Nature. 2010; 464:1357–1361. [PubMed: 20428172]

Fantuzzi G, Dinarello CA. Interleukin-18 and interleukin-1 beta: two cytokine substrates for ICE (caspase-1). J. Clin. Immunol. 1999; 19:1–11. [PubMed: 10080100]

Farese RV Jr. Walther TC. Lipid droplets finally get a little R-E-S-P-E-C-T. Cell. 2009; 139:855–860. [PubMed: 19945371]

Furuhashi M, Hotamisligil GS. Fatty acid-binding proteins: role in metabolic diseases and potential as drug targets. Nat. Rev. Drug Discov. 2008; 7:489–503. [PubMed: 18511927]

Grau V, Garn H, Holler J, Rose F, Blocher S, Hirschburger M, Fehrenbach H, Padberg W. Epidermal fatty acid-binding protein is increased in rat lungs following in vivo treatment with keratinocyte growth factor. Int. J. Biochem. Cell Biol. 2006; 38:279–287. [PubMed: 16256411]

Gregor MF, Hotamisligil GS. Inflammatory mechanisms in obesity. Annu. Rev. Immunol. 2011; 29:415–445. [PubMed: 21219177]

Hayes CS, Defeo K, Dang H, Trempus CS, Morris RJ, Gilmour SK. A prolonged and exaggerated wound response with elevated ODC activity mimics early tumor development. Carcinogenesis. 2011; 32:1340–1348. [PubMed: 21730362]

Hill JO, Wyatt HR, Peters JC. Energy balance and obesity. Circulation. 2012; 126:126–132. [PubMed: 22753534]

Hoffman HM, Rosengren S, Boyle DL, Cho JY, Nayar J, Mueller JL, Anderson JP, Wanderer AA, Firestein GS. Prevention of cold-associated acute inflammation in familial cold autoinflammatory syndrome by interleukin-1 receptor antagonist. Lancet. 2004; 364:1779–1785. [PubMed: 15541451]

Hume DA. Macrophages as APC and the dendritic cell myth. J. Immunol. 2008; 181:5829–5835. [PubMed: 18941170]

Jameson J, Havran WL. Skin gammadelta T-cell functions in homeostasis and wound healing. Immunol. Rev. 2007; 215:114–122. [PubMed: 17291283]

Joosten LA. Excessive interleukin-1 signaling determines the development of Th1 and Th17 responses in chronic inflammation. Arthritis Rheum. 2010; 62:320–322. [PubMed: 20112403]

Kastenmayer RJ, Fain MA, Perdue KA. A retrospective study of idiopathic ulcerative dermatitis in mice with a C57BL/6 background. J. Am. Assoc. Lab Anim Sci. 2006; 45:8–12. [PubMed: 17089984]

Khandekar MJ, Cohen P, Spiegelman BM. Molecular mechanisms of cancer development in obesity. Nat. Rev. Cancer. 2011; 11:886–895. [PubMed: 22113164]

L'homme L, Esser N, Riva L, Scheen A, Paquot N, Piette J, Legrand-Poels S. Unsaturated fatty acids prevent activation of NLRP3 inflammasome in human monocytes/macrophages. J. Lipid Res. 2013; 54:2998–3008. [PubMed: 24006511]

Li B, Reynolds JM, Stout RD, Bernlohr DA, Suttles J. Regulation of Th17 differentiation by epidermal fatty acid-binding protein. J. Immunol. 2009; 182:7625–7633. [PubMed: 19494286]

Lumeng CN, Bodzin JL, Saltiel AR. Obesity induces a phenotypic switch in adipose tissue macrophage polarization. J. Clin. Invest. 2007; 117:175–184. [PubMed: 17200717]

Maeda K, Uysal KT, Makowski L, Gorgun CZ, Atsumi G, Parker RA, Bruning J, Hertzel AV, Bernlohr DA, Hotamisligil GS. Role of the fatty acid binding protein mal1 in obesity and insulin resistance. Diabetes. 2003; 52:300–307. [PubMed: 12540600]

Makowski L, Brittingham KC, Reynolds JM, Suttles J, Hotamisligil GS. The fatty acid-binding protein, aP2, coordinates macrophage cholesterol trafficking and inflammatory activity. Macrophage expression of aP2 impacts peroxisome proliferator-activated receptor gamma and IkappaB kinase activities. J. Biol. Chem. 2005; 280:12888–12895. [PubMed: 15684432]

Mathur AN, Goebel L. Skin findings associated with obesity. Adolesc. Med. State Art. Rev. 2011; 22:146–56. ix. [PubMed: 21815449]

Mei S, Ni HM, Manley S, Bockus A, Kassel KM, Luyendyk JP, Copple BL, Ding WX. Differential roles of unsaturated and saturated fatty acids on autophagy and apoptosis in hepatocytes. J. Pharmacol. Exp. Ther. 2011; 339:487–498. [PubMed: 21856859]

Mirmirani P, Carpenter DM. Skin disorders associated with obesity in children and adolescents: a population-based study. Pediatr. Dermatol. 2014; 31:183–190. [PubMed: 24329996]

Murray PJ, Wynn TA. Protective and pathogenic functions of macrophage subsets. Nat. Rev. Immunol. 2011; 11:723–737. [PubMed: 21997792]

Nakahira K, Haspel JA, Rathinam VA, Lee SJ, Dolinay T, Lam HC, Englert JA, Rabinovitch M, Cernadas M, Kim HP, Fitzgerald KA, Ryter SW, Choi AM. Autophagy proteins regulate innate immune responses by inhibiting the release of mitochondrial DNA mediated by the NALP3 inflammasome. Nat. Immunol. 2011; 12:222–230. [PubMed: 21151103]

Namatame I, Tomoda H, Arai H, Inoue K, Omura S. Complete inhibition of mouse macrophage-derived foam cell formation by triacsin C. J. Biochem. 1999; 125:319–327. [PubMed: 9990129]

Netea MG, Simon A, van,d. V, Kullberg BJ, Van der Meer JW, Joosten LA. IL-1beta processing in host defense: beyond the inflammasomes. PLoS. Pathog. 2010; 6:e1000661. [PubMed: 20195505]

Ogawa E, Owada Y, Ikawa S, Adachi Y, Egawa T, Nemoto K, Suzuki K, Hishinuma T, Kawashima H, Kondo H, Muto M, Aiba S, Okuyama R. Epidermal FABP (FABP5) regulates keratinocyte differentiation by 13(S)-HODE-mediated activation of the NF- kappaB signaling pathway. J. Invest Dermatol. 2011; 131:604–612. [PubMed: 21068754]

Patsouris D, Li PP, Thapar D, Chapman J, Olefsky JM, Neels JG. Ablation of CD11c-positive cells normalizes insulin sensitivity in obese insulin resistant animals. Cell Metab. 2008; 8:301–309. [PubMed: 18840360]

Petrilli V, Dostert C, Muruve DA, Tschopp J. The inflammasome: a danger sensing complex triggering innate immunity. Curr. Opin. Immunol. 2007; 19:615–622. [PubMed: 17977705]

Scheinfeld NS. Obesity and dermatology. Clin. Dermatol. 2004; 22:303–309. [PubMed: 15475230]

Schulz C, Gomez PE, Chorro L, Szabo-Rogers H, Cagnard N, Kierdorf K, Prinz M, Wu B, Jacobsen SE, Pollard JW, Frampton J, Liu KJ, Geissmann F. A lineage of myeloid cells independent of Myb and hematopoietic stem cells. Science. 2012; 336:86–90. [PubMed: 22442384]

Shipman AR, Millington GW. Obesity and the skin. Br. J. Dermatol. 2011; 165:743–750. [PubMed: 21564065]

Smathers RL, Petersen DR. The human fatty acid-binding protein family: evolutionary divergences and functions. Hum. Genomics. 2011; 5:170–191. [PubMed: 21504868]

Stienstra R, Joosten LA, Koenen T, van TB, van Diepen JA, van den Berg SA, Rensen PC, Voshol PJ, Fantuzzi G, Hijmans A, Kersten S, Muller M, van den Berg WB, van RN, Wabitsch M, Kullberg BJ, van der Meer JW, Kanneganti T, Tack CJ, Netea MG. The inflammasome-mediated caspase-1 activation controls adipocyte differentiation and insulin sensitivity. Cell Metab. 2010; 12:593–605. [PubMed: 21109192]

Sundberg JP, Taylor D, Lorch G, Miller J, Silva KA, Sundberg BA, Roopenian D, Sperling L, Ong D, King LE, Everts H. Primary follicular dystrophy with scarring dermatitis in C57BL/6 mouse substrains resembles central centrifugal cicatricial alopecia in humans. Vet. Pathol. 2011; 48:513–524. [PubMed: 20861494]

Vandanmagsar B, Youm YH, Ravussin A, Galgani JE, Stadler K, Mynatt RL, Ravussin E, Stephens JM, Dixit VD. The NLRP3 inflammasome instigates obesity-induced inflammation and insulin resistance. Nat. Med. 2011a; 17:179–188. [PubMed: 21217695]

Vandanmagsar B, Youm YH, Ravussin A, Galgani JE, Stadler K, Mynatt RL, Ravussin E, Stephens JM, Dixit VD. The NLRP3 inflammasome instigates obesity-induced inflammation and insulin resistance. Nat. Med. 2011b; 17:179–188. [PubMed: 21217695]

Wang Y, Yang C, Mao K, Chen S, Meng G, Sun B. Cellular localization of NLRP3 inflammasome. Protein Cell. 2013; 4:425–431. [PubMed: 23609011]

Warden CH, Fisler JS. Comparisons of diets used in animal models of high-fat feeding. Cell Metab. 2008; 7:277. [PubMed: 18396128]

Wen H, Gris D, Lei Y, Jha S, Zhang L, Huang MT, Brickey WJ, Ting JP. Fatty acid-induced NLRP3-ASC inflammasome activation interferes with insulin signaling. Nat. Immunol. 2011; 12:408–415. [PubMed: 21478880]

Wentworth JM, Naselli G, Brown WA, Doyle L, Phipson B, Smyth GK, Wabitsch M, O'Brien PE, Harrison LC. Pro-inflammatory CD11c+CD206+ adipose tissue macrophages are associated with insulin resistance in human obesity. Diabetes. 2010; 59:1648–1656. [PubMed: 20357360]

Williams LK, Csaki LS, Cantor RM, Reue K, Lawson GW. Ulcerative dermatitis in C57BL/6 mice exhibits an oxidative stress response consistent with normal wound healing. Comp Med. 2012; 62:166–171. [PubMed: 22776048]

Yan Y, Jiang W, Spinetti T, Tardivel A, Castillo R, Bourquin C, Guarda G, Tian Z, Tschopp J, Zhou R. Omega-3 fatty acids prevent inflammation and metabolic disorder through inhibition of NLRP3 inflammasome activation. Immunity. 2013; 38:1154–1163. [PubMed: 23809162]

Yosipovitch G, DeVore A, Dawn A. Obesity and the skin: skin physiology and skin manifestations of obesity. J. Am. Acad. Dermatol. 2007; 56:901–916. [PubMed: 17504714]

Zhang Y, Sun Y, Rao E, Yan F, Li Q, Zhang Y, Silverstein KA, Liu S, Sauter E, Cleary MP, Li B. Fatty acid binding protein E-FABP restricts tumor growth by promoting IFNbeta responses in tumor-associated macrophages. Cancer Res. 2014; 74:2987–2998.

Highlights

1. Consumption of a high-fat diet (HFD) induces inflammatory skin lesions
2. HFD promotes CD11c+ macrophage infiltration and NLRP3 inflammasome activation
3. E-FABP couples lipid transportation and IL-1β/IL-18 production
4. Deficiency of E-FABP protects mice against HFD-induced skin inflammation

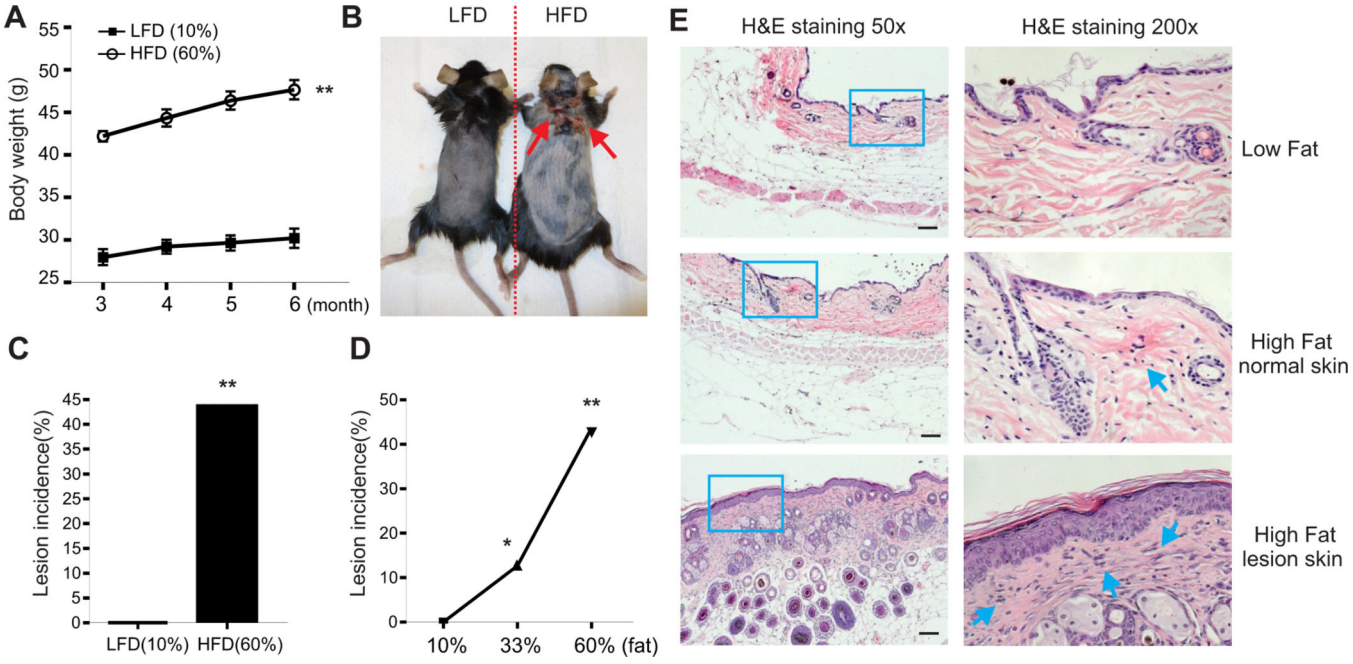

Figure 1. HFD induces inflammatory skin lesions in mice

(A) C57BL/6 mice were grouped and fed the HFD (60% fat) and the LDF (10% fat) (n=16/group), respectively. Average body weight of each group was shown from 3 months to 6 months on special diets (**, $p<0.01$).

(B) Representative pictures of a LFD-fed mouse and a HFD-induced lesion mouse.

(C) Skin lesion incidence in mice fed with the LFD or the HFD for 9 months (n=16/group) (**, $p<0.01$).

(D) Skin lesion incidence in mice with 10% fat diet (n=60), 33% fat diet (n=63) and 60% fat diet (n=21) for 9 months (*, $p<0.05$; **, $p<0.01$)

(E) Hematoxylin and eosin (H&E) staining of skin tissues from LFD-fed mice, normal HFD-fed mice and lesional HFD-fed mice. Scale bars represent 100μM.

Data are shown as mean ± SEM and representative of two to three experiments.

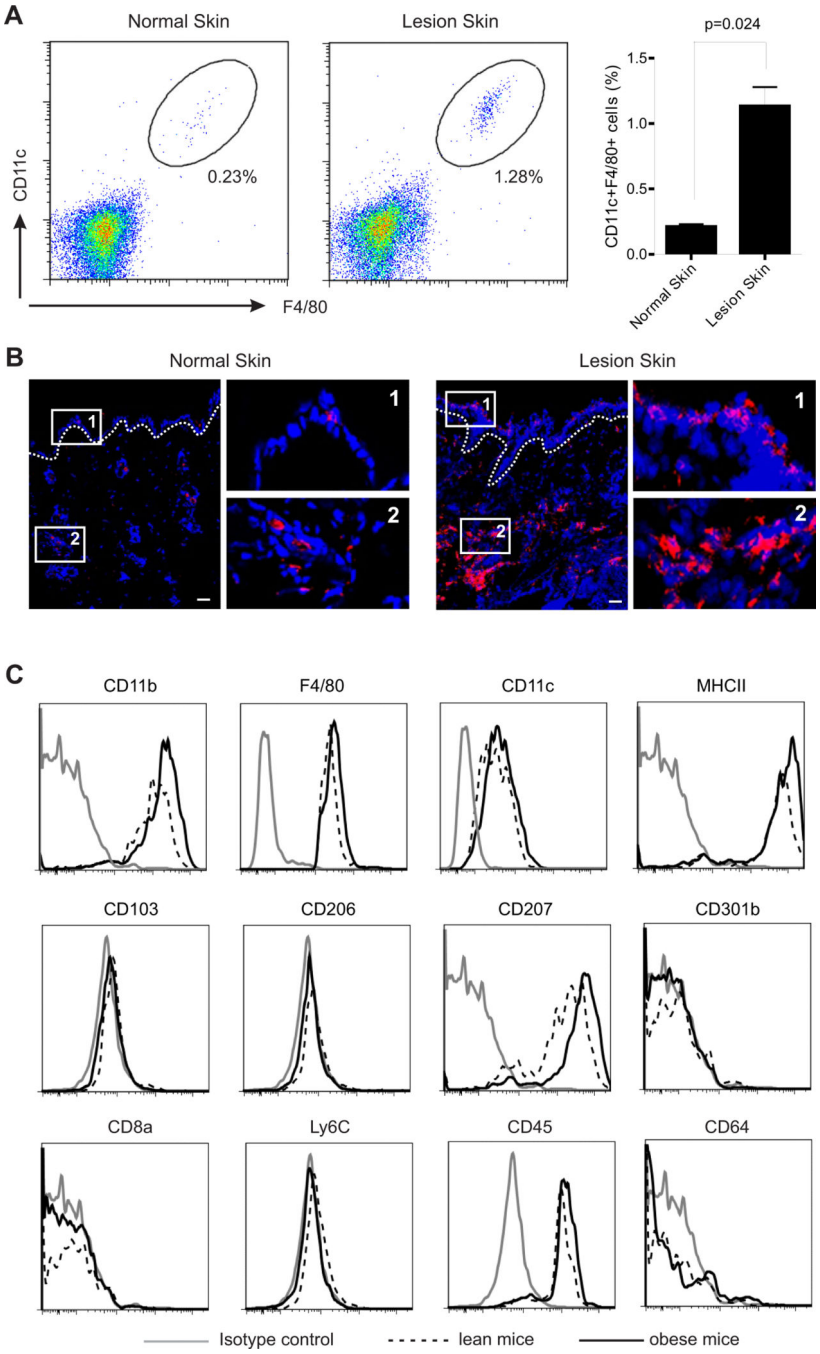

Figure 2. HFD promotes the accumulation of CD11c$^+$ macrophages in obese mice

(A) Analysis of the accumulation of CD11c$^+$ macrophages in skin tissues from LFD-fed normal mice and HFD-fed lesion mice by flow cytometry. Average percentage of CD11c$^+$ macrophages in skin is shown in the right panel.

(B) Frozen sections of skin tissues from LFD-fed normal mice and HFD-fed lesion mice were stained with F4/80 mAb (red) and DAPI (blue) for confocal microscopy analysis. Magnified fields of selected areas are shown in the right panel. Scale bars represent 10μM.

(C) Phenotypic characterization of HFD-elevated skin macrophages by flow cytometric analysis.

Data are shown as mean ± SEM and representative of at least three experiments. See also Figure S1.

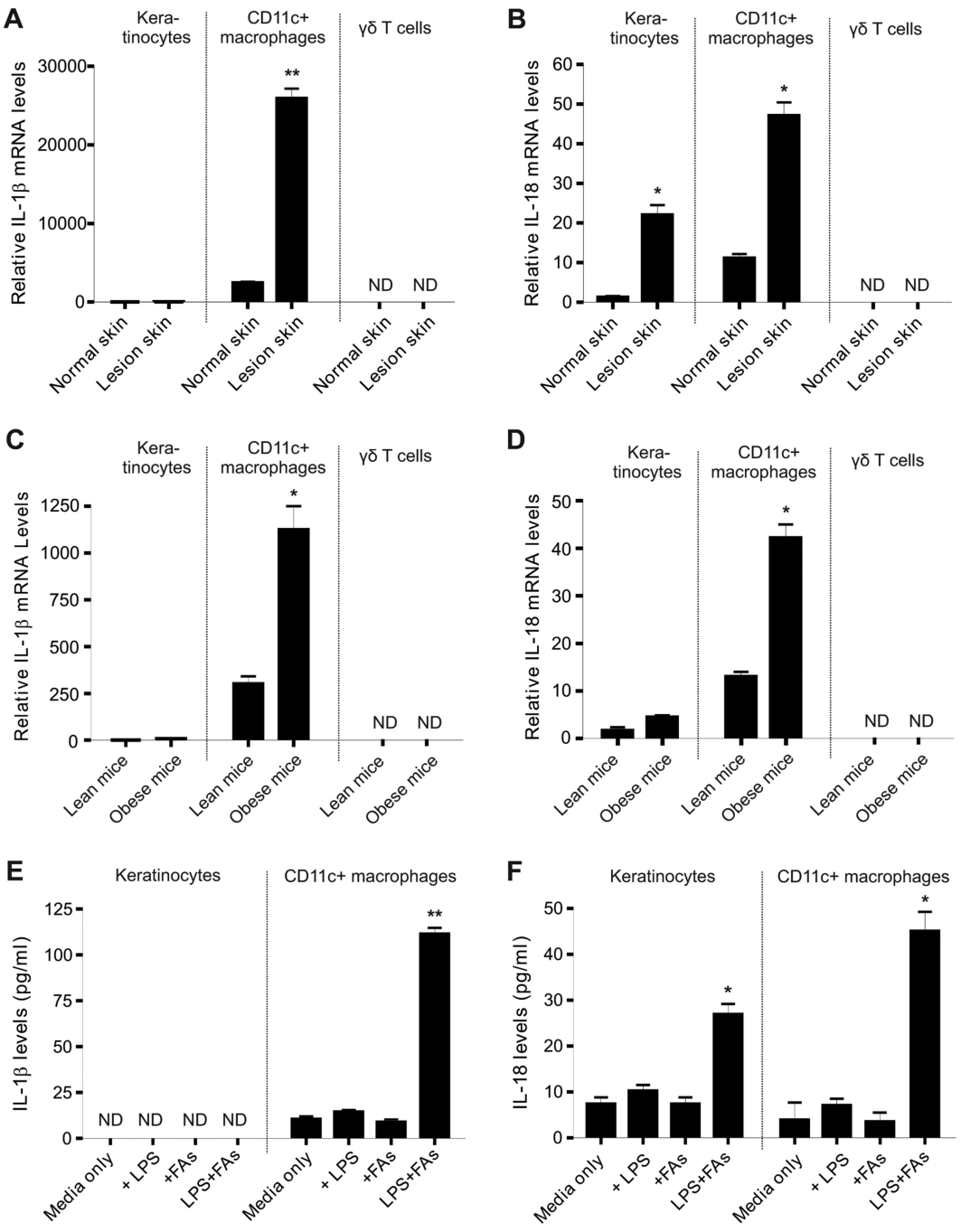

Figure 3. Upregulation of IL-1β and IL-18 production in HFD-induced skin lesions

(A-B) Keratinocytes, CD11c$^+$ macrophages and γδ T cells were separated by a flow sorter from either normal skin tissues or HFD-induced lesional skin tissues. Relative levels of IL-1β mRNA (A) and IL-18 mRNA (B) were determined by quantitative real-time PCR (*, $p<0.05$; **, $p<0.01$).

(C-D) Keratinocytes, CD11c$^+$ macrophages and γδ T cells were separated by a flow sorter from feltwheel-induced lesional skin tissues from lean or obese mice. Relative levels of

IL-1β mRNA (A) and IL-18 mRNA (B) were determined by quantitative real-time PCR (*, $p<0.05$).

(E-F) Measurement of IL-1β (E) and IL-18 (F) by ELISA in supernatants of primary keratinocytes or $CD11c^+$ macrophages stimulated with designated conditions for 24 hours (LPS, 100ng/ml, FAs, 200μM palmitate) (*, $p<0.05$; **, $p<0.01$).

Data are shown as mean ± SEM and representative of at least three experiments. See also Table S1 and Figure S2.

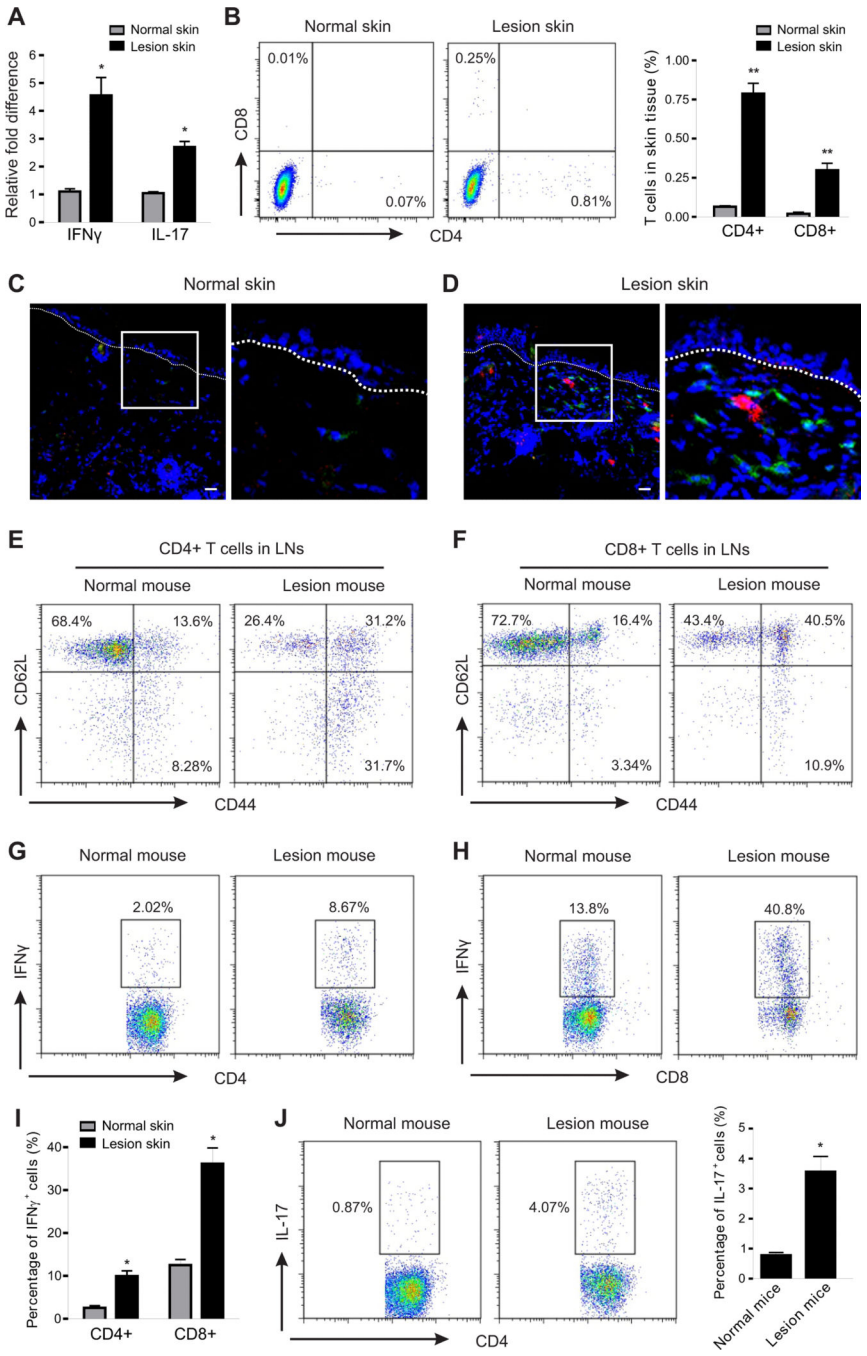

Figure 4. HFD-induced lesions are associated with enhanced T cell activation

(A) Analysis of the relative mRNA levels of IFNγ and IL-17 in skin tissues from LFD-fed normal mice and HFD-fed lesion mice by real-time PCR (*, $p<0.05$).

(B) Flow cytometric analysis for $CD4^+$ T cells and $CD8^+$ T cells in skin epidermis of LFD-fed normal mice and HFD-fed lesion mice. Average percentage of T cells in skin epidermis is shown in the right panel (**, $p<0.01$).

(C-D) Frozen sections of skin tissues from LFD-fed normal mice and HFD-fed lesion mice were stained with CD4 mAb (green), CD8 mAb (red) and DAPI (blue) for confocal

microscopic analysis. Magnified fields of selected areas are shown in the right panel of each figure. Scale bars represent 10μM.

(E-F) Flow cytometric analysis of the activation status of $CD4^+$ T cells (E) and $CD8^+$ T cells (F) in draining lymph nodes (LNs) from LFD-fed normal mice and HFD-fed lesion mice. Data represent one of three independent experiments with similar results.

(G-I) Analysis of IFNγ production in $CD4^+$ T cells (G) and $CD8^+$ T cells (H) of draining LNs from LFD-fed normal mice and HFD-fed lesion mice by intracellular staining. Average percentage of $IFN\gamma^+$ cells in total $CD4^+$ or $CD8^+$ T cells is shown in panel I (*, $p<0.05$).

(J) Analysis of IL-17 production in $CD4^+$ T cells of draining LNs from LFD-fed normal mice and HFD-fed lesion mice lesions by intracellular staining. Average percentage of $IL\text{-}17^+$ cells in total $CD4^+$ T cells is shown in the right panel (*, $p<0.05$).

Data are shown as mean ± SEM and representative of three experiments. See also Figure S3.

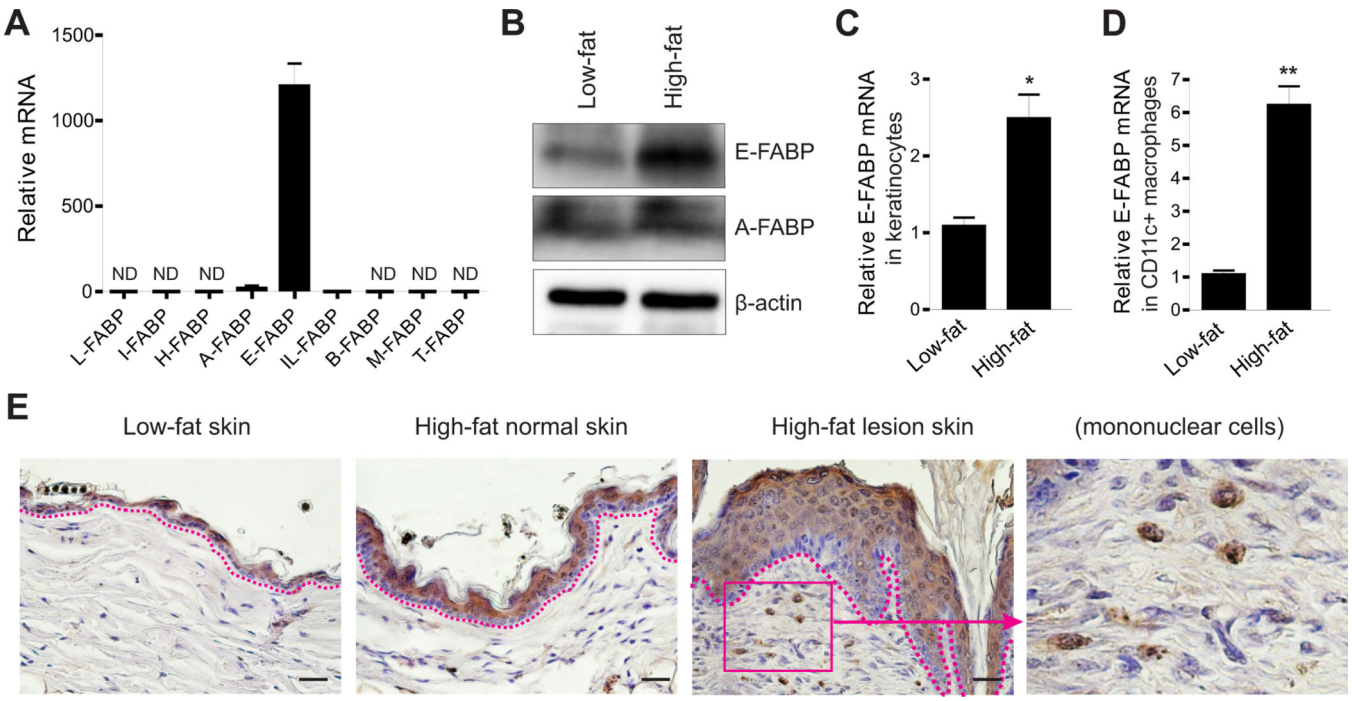

Figure 5. HFD enhances E-FABP expression in skin tissues

(A) Analysis of the profile of FABP family in normal skin tissues by real-time PCR.

(B) Western blotting for E-FABP and A-FABP expression in skin tissues from mice fed the LFD or the HFD for 6 months.

(C) Analysis of E-FABP expression in purified keratinocytes from mice fed the LFD or the HFD for 6 months (*, $p<0.05$)

(D) Analysis of E-FABP expression in purified $CD11c^{+}$ macrophages from skin tissues of mice fed the LFD or the HFD for 6 months (**, $p<0.01$)

(E) Immunohistochemistry (IHC) staining of E-FABP expression (brown color) in paraffin-embedded skin sections from mice fed the LFD or the HFD with/without skin lesions. Hematoxylin was applied for counter staining (blue color). (Scale bars represent 25μM. LFD means 10% fat, HFD means 60% fat)

Data are shown as mean ± SEM and representative of three experiments. See also Figure S4.

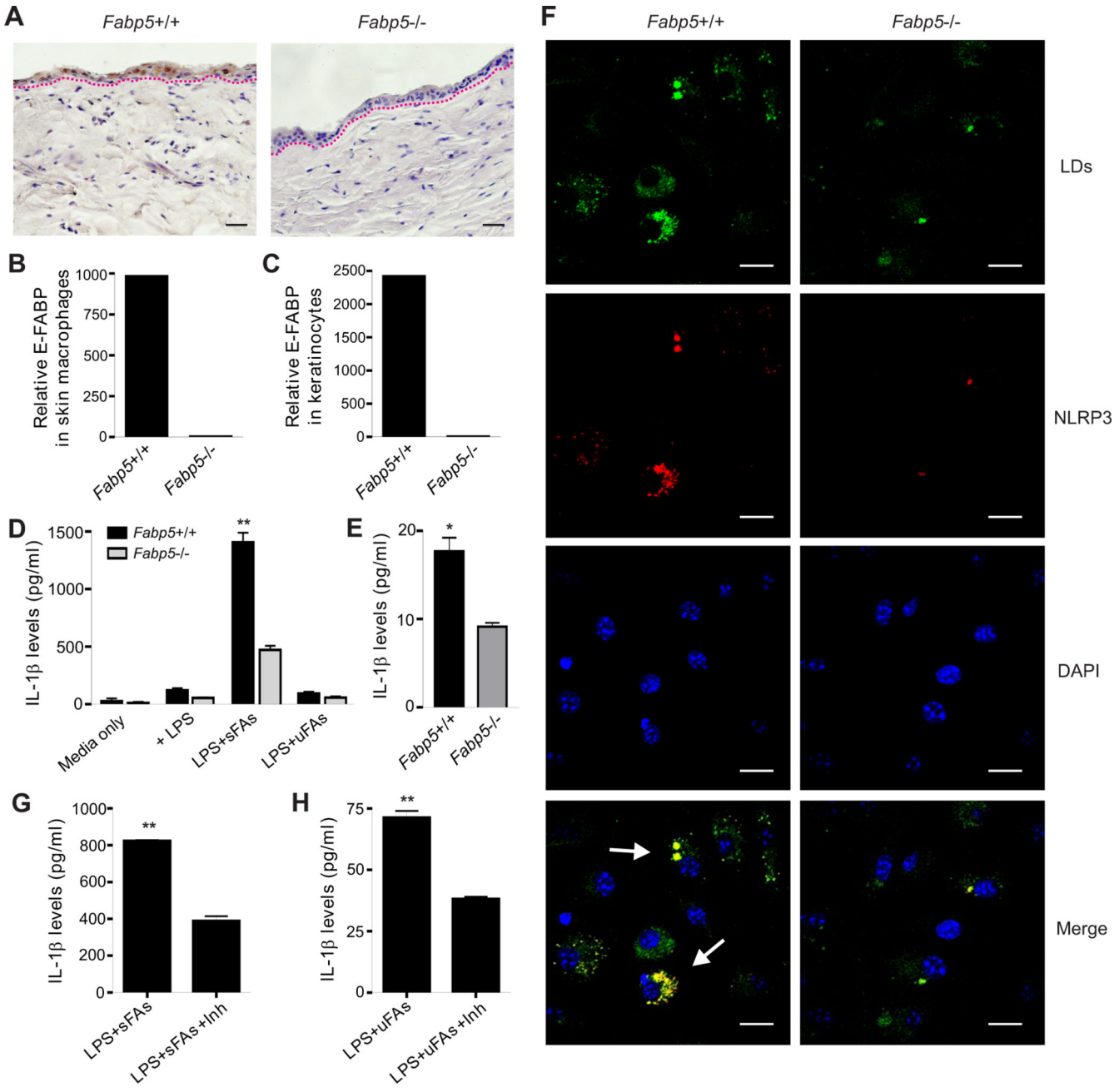

Figure 6. Expression of E-FABP facilitates FA-induced inflammasome activation and cytokine production in macrophages

(A) IHC staining of E-FABP expression in paraffin-embedded skin tissues from *Fabp5*$^{+/+}$ mice and *Fabp5*$^{-/-}$ mice. Scale bars represent 25μM.

(B-C) Analysis of E-FABP levels in flow-sorted CD11c^{+} macrophages (B) and keratinocytes (C) from *Fabp5*$^{+/+}$ mice and *Fabp5*$^{-/-}$ mice.

(D) Measurement of IL-1β levels in supernatants of resting or LPS-primed bone-marrow derived-CD11c^{+} macrophages (1×10^{6}) stimulated with or without saturated FA (palmitate, 200μM) or unsaturated FAs (oleate/linoleate, 200μM) by ELISA (**, $p<0.01$).

(E) Measurement of IL-1β levels in supernatants of LPS-primed skin $CD11c^+$ macrophages (2×10^4) stimulated with or without saturated FA (palmitate, 200μM) by ELISA (*, $p<0.05$).
(F) LPS-primed bone-marrow derived-$CD11c^+$ macrophages were treated with palmitate for 16h and stained for lipid droplet formation (BODIPY, green), NLRP3 expression (red color) and nuclei (DAPI, blue) by confocal microscopy. Scale bars represent 10μM.
(G) ELISA for IL-1β levels in the supernatants of LPS-primed, palmitate-treated $CD11c^+$ macrophages (1×10^6) in the presence of LD inhibitor Triacsin C (2.5μM) (**, $p<0.01$).
(H) ELISA for IL-1β levels in the supernatants of LPS-primed, oleate/linoleate-treated $CD11c^+$ macrophages (1×10^6) in the presence of LD inhibitor Triacsin C (2.5μM) (**, $p<0.01$).
Data are shown as mean ± SEM and representative of three experiments. See also Figure S5.

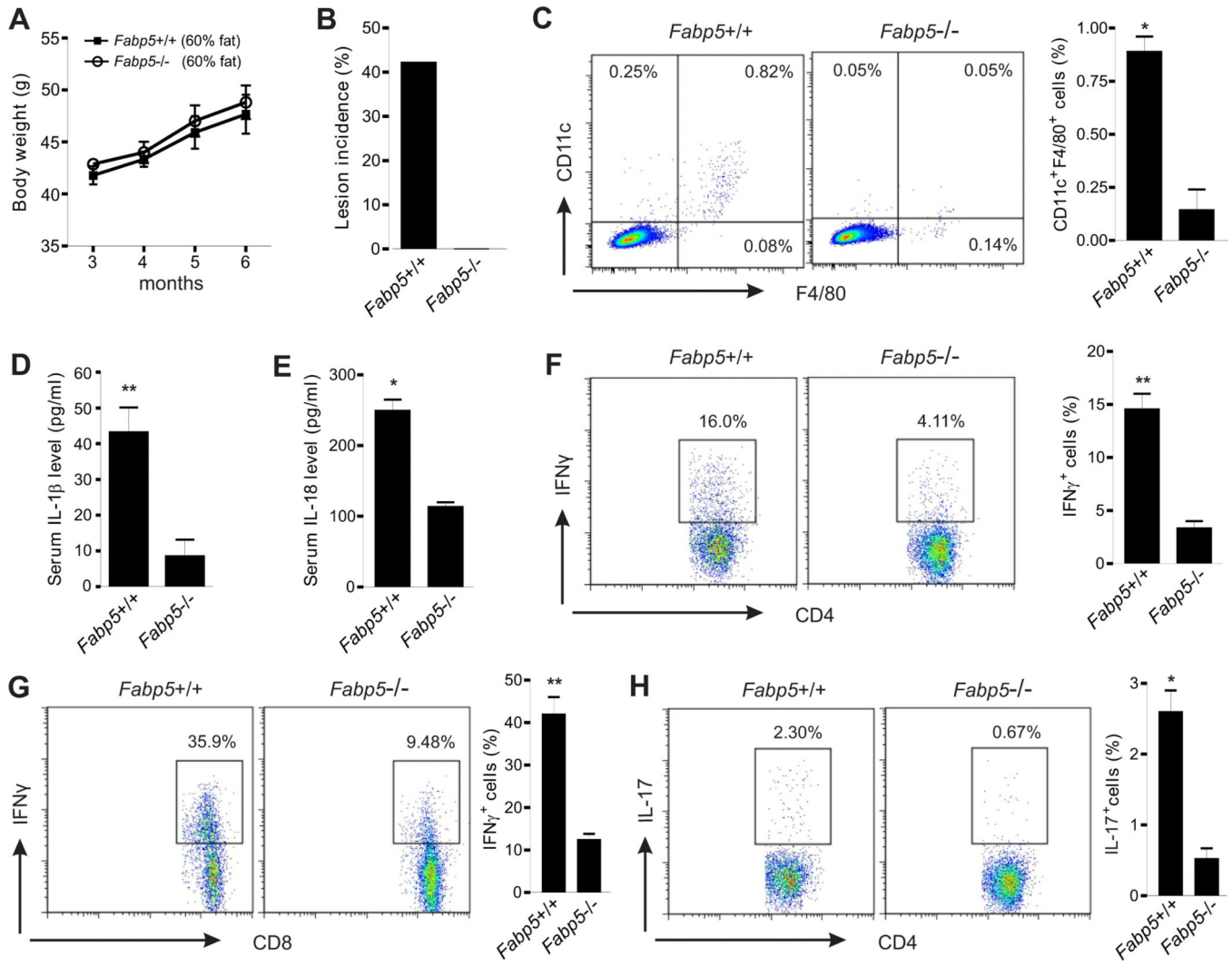

Figure 7. E-FABP deficiency protects mice from development of HFD-induced skin inflammation

(A) Average body weight of *Fabp5*$^{+/+}$ and *Fabp5*$^{-/-}$ mice was shown from 3 months to 6 months on the HFD (n=21/group).

(B) Skin lesion incidence in *Fabp5*$^{+/+}$ mice and *Fabp5*$^{-/-}$ mice after nine month feeding with the HFD (n=21/group).

(C) Flow cytometric analysis of the infiltration of CD11c^{+}F4/80^{+} macrophages in skin epidermis from *Fabp5*$^{+/+}$ or *Fabp5*$^{-/-}$ mice fed the HFD for six months. Average percentage of CD11c^{+}F4/80^{+} macrophages is shown in the right panel (*, p<0.05).

(D) ELISA for IL-1β levels in the serum of *Fabp5*$^{+/+}$ or *Fabp5*$^{-/-}$ mice fed the HFD for six months (**, p<0.01).

(E) ELISA for IL-18 levels in the serum of *Fabp5*$^{+/+}$ or *Fabp5*$^{-/-}$ mice fed the HFD for six months (*, p<0.05).

(F-G) Analysis of IFNγ production in CD4^{+} T cells (F) and CD8^{+} T cells (G) of draining LNs from *Fabp5*$^{+/+}$ or *Fabp5*$^{-/-}$ mice fed the HFD for six months by intracellular staining.

Average percentage of IFNγ^+ cells in total CD4$^+$ or total CD8$^+$ T cells is respectively shown in the right panel (**, $p<0.01$).

(H) Analysis of IL-17 production in CD4$^+$ T cells of draining LNs from *Fabp5*$^{+/+}$ or *Fabp5*$^{-/-}$ mice fed the HFD for six months by intracellular staining. Average percentage of IL-17$^+$ cells is shown in the right panel (*, $p<0.05$).

Data are shown as mean ± SEM and representative of three experiments. See also Figure S6.